Quality of a 28 cm Long LYSO Crystal and Progress on Optical and Scintillation Properties

Rihua Mao, *Member, IEEE*, Liyuan Zhang, *Member, IEEE*, and Ren-Yuan Zhu, *Senior Member, IEEE*

***Abstract*—Because of their high stopping power and fast and bright scintillation, cerium doped LSO and LYSO crystals have attracted a broad interest in the physics community pursuing precision electromagnetic calorimeter for future high energy physics experiments. Their excellent radiation hardness against γ-rays, neutrons and charged hadrons also makes them a preferred material for calorimeters to be operated in a severe radiation environment, such as the HL-LHC. An effort was made at SIPAT to grow 25 X_0 (28 cm) long LYSO crystals for high energy physics applications. In this paper, the optical and scintillation properties and its radiation hardness against γ-ray irradiations up to 1 Mrad are presented for the first $2.5 \times 2.5 \times 28$ cm LYSO sample. An absorption band was found at the seed end of this sample and three other long samples, which was traced back to a bad seed crystal used in the corresponding crystal growth process. Significant progresses in optical and scintillation properties were achieved for large size LYSO crystals after eliminating this absorption band.**

***Index Terms*—Crystal, light output, lutetium oxyorthosilicate, lutetium yttrium oxyorthosilicate, photo-luminescence, radiation damage, scintillator, transmission.**

I. Introduction

In the last two decades, cerium doped silicate based heavy crystal scintillators have been developed for the medical industry. As of today, mass production capabilities of lutetium oxyorthosilicate (LSO) [1] and lutetium-yttrium oxyorthosilicate (LYSO) [2], [3] are established. Because of their high stopping power ($\rho = 7.4$ g/cm^3, $\mathrm{X}_0 = 1.14$ cm and $\mathrm{R}_{Moliere} = 2.07$ cm), high light yield (about 4 times of BGO) and fast decay time ($\tau =\sim 40$ ns) these crystals have also attracted a broad interest in the physics community for future high energy physics experiments [4], such as a super B factory [5] and the international linear collider (ILC) [6]. Investigations on large size ($2.5 \times 2.5 \times 20$ cm) LSO/LYSO crystals also show that this new generation of inorganic crystal scintillators has excellent radiation hardness against γ-rays [7], neutrons [8] and charged hadrons [9]. This material thus may also be considered for calorimeters to be operated in a severe radiation environment, such as the HL-LHC, and seems the only suitable scintillator for which mass-production capability is presently available.

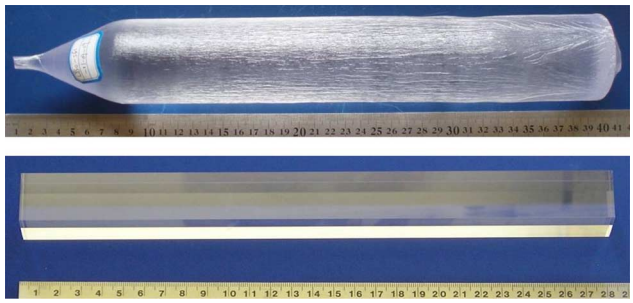

Fig. 1. Top: A LYSO ingot grown by SIPAT with constant diameter of 60 mm and 310 mm long (top). Bottom: The first 25 X_0 long LYSO sample of $25 \times 25 \times 280$ mm cut from the ingot.

The main obstacles of using this material in the experimental physics are two fold: the availability of high quality crystals in sufficiently large size and the high cost associated with their raw material cost and high melting point ($> 2{,}000$°C). An effort has been made at Sichuan Institute of Piezoelectric and Acousto-optic Technology (SIPAT), Chongqing, China, to grow large size (up to 28 cm or 25 X_0 long) LSO and LYSO crystals for high energy physics applications. In this work, the first $2.5 \times 2.5 \times 28$ cm LYSO sample from SIPAT is evaluated, including its optical and scintillation properties and its radiation hardness against γ-rays up to 1 Mrad. Poor longitudinal transmittance was observed in this sample, which was found to be caused by an absorption band at the seed end. After removing this absorption band both the optical and scintillation properties are improved significantly for large size samples.

Section II describes the optical and scintillation properties of the first 28 cm long sample. Its radiation hardness against γ-ray irradiations up to 1 Mrad is presented in Section III. Section IV shows the progress in optical and scintillation properties for large size LYSO crystals. A brief summary is given in Section V.

II. First 28 cm long LYSO Sample

Fig. 1 is a photo showing a LYSO ingot (top) and the first $2.5 \times 2.5 \times 28$ cm LYSO sample (bottom) grown at SIPAT. The diameter of the ingot is about 60 mm and the length of the constant diameter is about 310 mm. From this ingot the first 28 cm long LYSO sample (SIPAT-LYSO-L7) was obtained.

All six surfaces of the sample are polished. Its dimension is found to be within 100 μm tolerance to the nominal values. The sample is colorless, crack free, without any visible inclusion. No thermal treatment was applied before the initial measurements. According to the manufacturer, the yttrium concentration is about 7%. The nominal cerium doping level is about 0.2%.

Manuscript received November 04, 2011; revised December 23, 2011; accepted December 28, 2011. This work was supported in part by the U.S. Department of Energy under grant DE-FG03-92-ER-40701 and the U.S. National Science Foundation Award PHY-0612805.

The authors are with the California Institute of Technology, Pasadena, CA 91125 USA (e-mail: zhu@hep.caltech.edu).

Color versions of one or more of the figures in this paper are available online at http://ieeexplore.ieee.org.

Digital Object Identifier 10.1109/TNS.2012.2184302

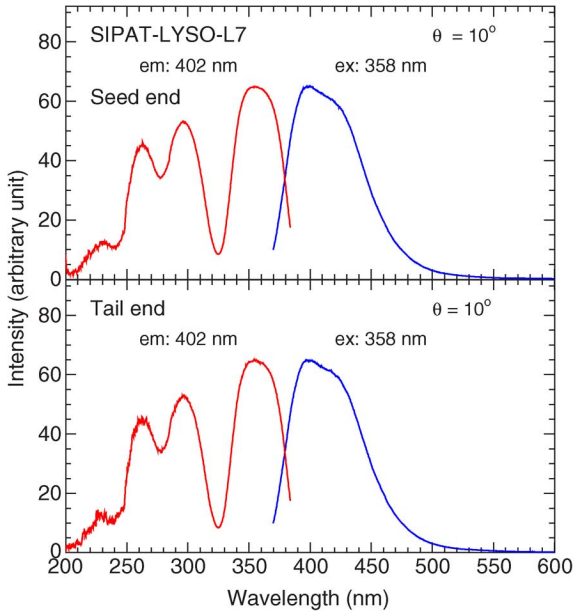

Fig. 2. Excitation (red) and photo-luminescence (blue) spectra are shown as a function of wavelength for SIPAT-LYSO-L7.

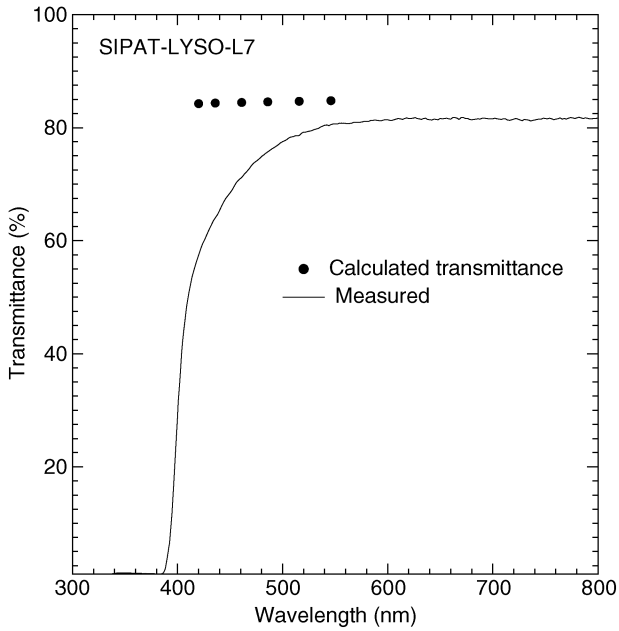

Fig. 3. Longitudinal transmittance spectrum (black lines) is shown as a function of wavelength for SIPAT-LYSO-L7 together with the theoretical limits (black dots).

The actual cerium concentration in the sample, however, would be less than the nominal value because of the cerium segregation. The distribution of the cerium concentration along the long sample's axis is not uniform.

The UV excited photo-luminescence spectra at two ends of the sample were measured by a Hitachi F-4500 fluorescence spectrophotometer. The angle between the sample normal and the excitation beam is set to be 10° to avoid internal absorption of the crystal [10]. Fig. 2 shows the excitation (red lines) and photo-luminescence (blue lines) spectra measured at the seed (top) and tail (bottom) end of SIPAT-LYSO-L7. Both the excitation and emission spectra are consistent between these two ends, indicating no deviation of scintillation along the crystal.

The longitudinal and transverse transmittance spectra were measured using a Perkin Elmer Lambda 950 spectrophotometer equipped with double beam, double monochromator and a general purpose optical bench (GPOB) with light path up to 40 cm. The systematic uncertainty in repeated measurements is about 0.15%.

Fig. 3 shows the longitudinal transmittance spectrum (black line) for SIPAT-LYSO-L7. Also shown in this figure are the theoretical limits of the transmittance (black dots) calculated by using the refractive index of LYSO [10]. Taking into account multiple bouncing between two end surfaces the theoretical limits of the transmittance without internal absorption can be calculated as [11]

$$\begin{aligned} T_s &= (1-R)^2 + R^2(1-R)^2 + \ldots \\ &= (1-R)/(1+R) \end{aligned} \tag{1}$$

where

$$R = \frac{(n_{crystal} - n_{air})^2}{(n_{crystal} + n_{air})^2} \tag{2}$$

where $\mathrm{n}_{crystal}$ and n_{air} are the refractive index of crystal and air respectively, which is a function of wavelength.

A comparison of the measured optical transmittance and its theoretical limit reveals sample's overall optical quality. Poor transmittance was found between 400 nm and 600 nm. Fig. 4 shows the transverse transmittance spectra measured every 2 cm from the seed (curve-1) to the tail (curve-13) end. A large divergence of the transverse transmittance spectra between 400 and 600 nm is observed. The insert shows an expanded view between 420 nm and 450 nm, illustrating clearly the degradation of transmittance from the tail end to the seed end. While the transverse transmittance measured at 2 cm from the tail end (curve-13) is very good, that measured at 2 cm from the seed end is rather poor. From these spectra alone one can not judge if the poor transmittance observed at the seed end is caused by internal absorption or scattering. Also shown in this figure is the cut-off wavelength for the transverse transmittance. It is defined as the wavelength at which the transmittance value is 50% of the theoretical value at 600 nm. From the numerical values of the cut-off wavelength one may extract the cerium concentration by using an established correlation. This will be discussed in our future publication.

Despite the poor transmittance observed at the seed end this 28 cm long LYSO sample provides adequate light output and energy resolution. Two photodetectors, a Hamamatsu R1306 PMT and a Hamamatsu S8664-1010 APD with 1 cm^2 area, were used in the light output measurement. In these measurements the seed end of the sample was coupled to the PMT via Dow Corning 200 fluid, while all other faces of the sample were wrapped with two layers of Tyvek paper. To reduce the effect of the intrinsic natural radioactivity, a collimated $^{22}\mathrm{Na}$ source was used with a coincidence trigger provided by a BaF_2 crystal. The detail of the setup used in these measurements is discussed

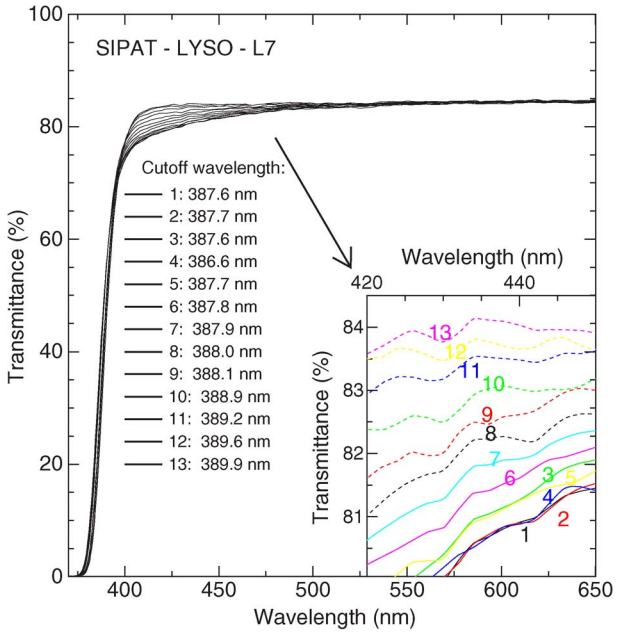

Fig. 4. Transverse transmittance spectra measured every 2 cm from the seed (curve-1) to the tail (curve-13) end are shown as a function of wavelength for SIPAT-LYSO-L7. The inset is an expanded view between 420 nm and 450 nm.

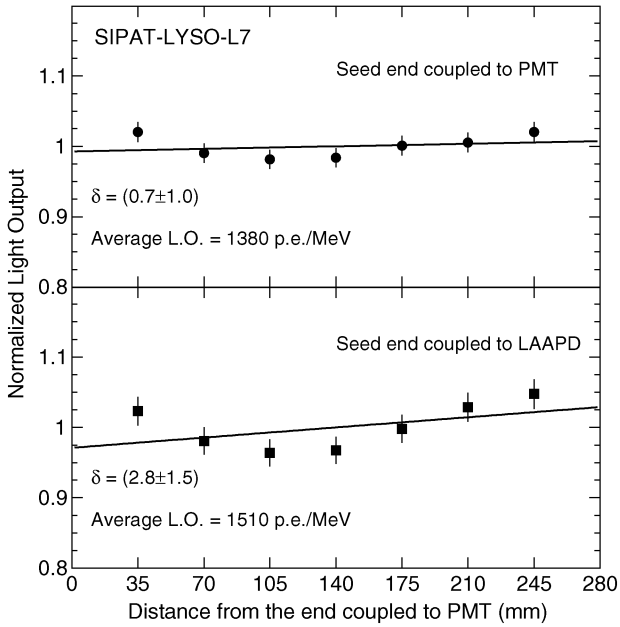

Fig. 6. Normalized light output (black dots) is shown as a function of distance to the photo-detector for SIPAT-LYSO-L7. Also shown are the linear fit and corresponding average light output and light response uniformity (δ) as defined in equation (3).

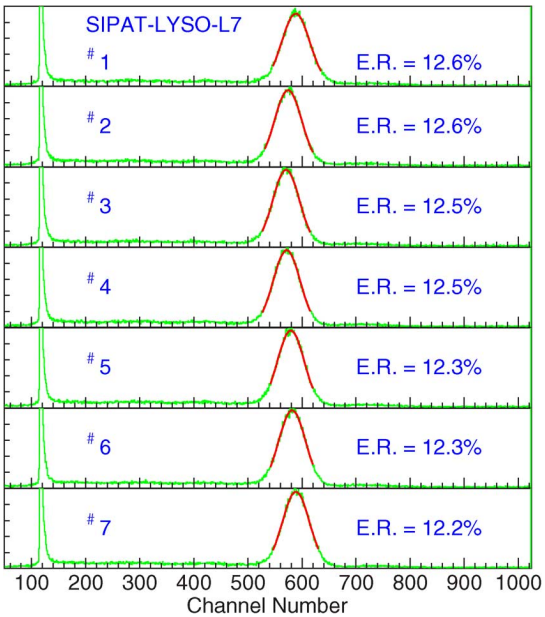

Fig. 5. Pulse height spectra of 0.511 MeV γ-ray peaks (green lines) and corresponding Gaussian fits (red lines) measured by a Hamamatsu R1306 PMT are shown at seven points evenly distributed along SIPAT-LYSO-L7. Also shown are the numerical values of the FWHM energy resolutions (E.R.).

in [6]. The γ-ray peak position was determined by a simple Gaussian fit. Fig. 5 shows the pulse height spectra measured by the Hamamatsu R1306 PMT at seven points evenly distributed along SIPAT-LYSO-L7. The FWHM resolutions obtained for 0.511 MeV γ-rays from the ^{22}Na source are about 12.5%, which is quite good for crystals of such length.

The γ-ray peak positions obtained by sending a collimated beam of γ-ray at seven points evenly distributed along the crystal were used to extract the light response uniformity of the crystal. A linear fit is used to fit the normalized response

$$\frac{LO}{LO_{mid}} = 1 + \delta \frac{x}{x_{mid} - 1} \tag{3}$$

where LO_{mid} represents the average light output at the middle of the sample, x is the distance from the end coupled to the readout device and δ represents the deviation of the light response uniformity.

Fig. 6 shows the normalized light output (black dots) as a function of the distance to the photo-detector, measured by the Hamamatsu 1306 PMT (top) and the Hamamatsu S8664-1010 APD (bottom) for SIPAT-LYSO-L7. The average light output and the light response uniformity (δ) are also shown in this figure. The numerical values of the average light output are 1,380 p.e./MeV and 1,510 p.e./MeV for the PMT and APD readout respectively. The corresponding light response uniformities (δ values) are 0.7 $\pm$1% and 2.8 $\pm$1.5%. Despite its poor transmittance observed at the seed end this 28 cm long LYSO sample shows rather good longitudinal light response uniformity.

III. Radiation Resistance Against γ-Ray Irradiations

Radiation damage of this sample against γ-rays was investigated. A ^{137}Cs source was used for the irradiations with a dose rate of 7,500 rad/h. The irradiation was carried out step by step to integrated doses of 10^2, 10^4 and 10^6 rad. Since radiation damage in LYSO crystals does not recover, and is not dose rate dependent [7], the total integrated dose is used to represent the level of the radiation applied to this sample in this study.

Fig. 7 shows an expanded view of the longitudinal transmittance spectra before and after the γ-ray irradiations with an integrated dose of 10^2, 10^4 and 10^6 rad. Also shown in the figure is

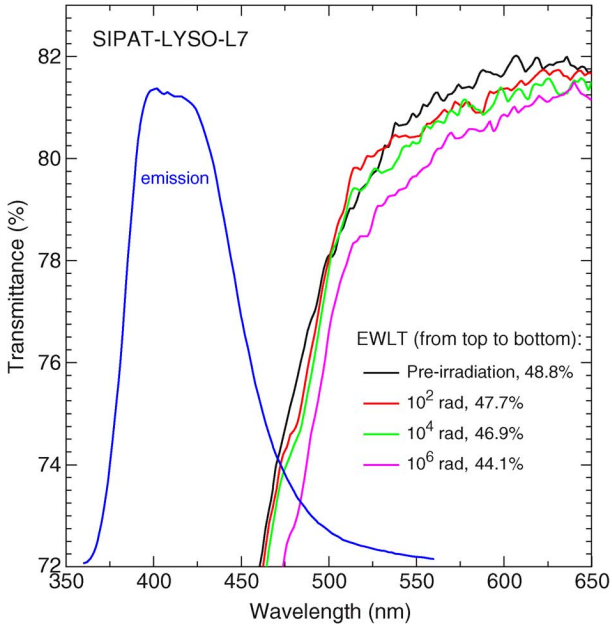

Fig. 7. Expanded view of the longitudinal transmittance spectra measured before and after γ-ray irradiations in several steps up to 1 Mrad is shown for SIPAT-LYSO-L7. Also shown is the emission spectrum and the values of EWLT defined in the text.

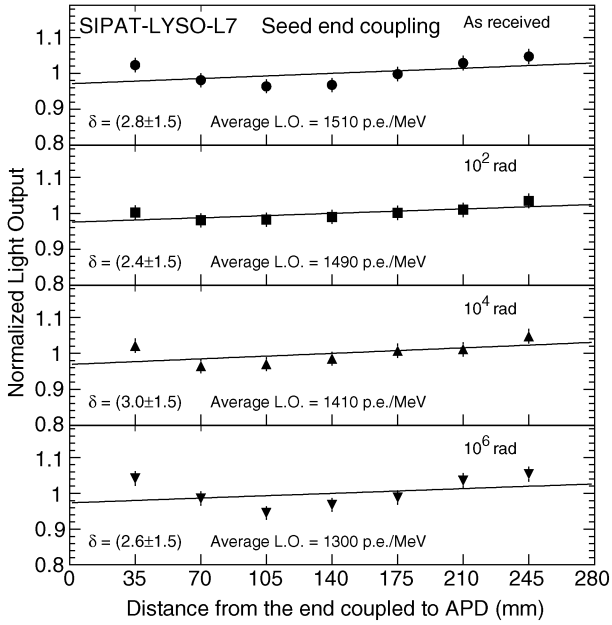

Fig. 8. Normalized light output and light response uniformity measured by Hamamatsu S8664-1010 APD before and after γ-ray irradiations in several steps up to 1 Mrad are shown for SIPAT-LYSO-L7.

the emission spectrum and the values of the emission weighted longitudinal transmittance (EWLT), which is defined as

$$EWLT = \frac{\int LT(\lambda)Em(\lambda)d\lambda}{\int Em(\lambda)d\lambda}. \quad (4)$$

The numerical value of EWLT represents how transparent the crystal is to the scintillation light so is a good measure of its transparency. Its degradation represents the radiation damage effect on transparency. For SIPAT-LYSO-L7 its radiation damage in EWLT is 9.6% after 1 Mrad irradiations.

Fig. 8 shows the normalized light output and response uniformity measured by the Hamamatsu APD before and after γ-ray irradiations with an integrated dose of 10^2, 10^4 and 10^6 rad. The damage on the light output was found to be about 13% after 1 Mrad irradiations. This is much better than 26% light output loss measured for typical lead tungstate (PWO) crystals after 10 krad with a dose rate of 400 rad/h [12]. We also note that the light response uniformity of SIPAT-LYSO-L7 does not change, indicating that its energy resolution may be maintained even after 1 Mrad irradiations. Despite the poor transmittance at the seed end the radiation resistance of this 28 cm long LYSO sample SIPAT-LYSO-L7 is quite good.

IV. Progress on Optical and Scintillation Properties

Since the poor transmittance between 400 nm and 600 nm observed in SIPAT-LYSO-L7 reduces its light output it therefore should be eliminated. Similar poor transmittance was also found in other three LYSO samples of 20 cm long grown at SIPAT for a SuperB beam test: SIPAT-LYSO-L8, L9 and L10. Their longitudinal and transverse spectra were found to be similar to that shown in Figs. 3 and 4 respectively with poor transmittance located at the seed end.

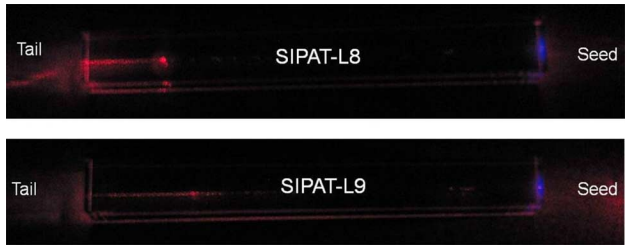

Fig. 9. Picture showing scattering centers exists at the tail end of SIPAT-LYSO-L8 and SIPAT-LYSO-L9.

Poor transmittance may be caused by point defects which absorb light in the crystal. It may also be caused by scattering centers introduced by macroscopic defects, such as cracking and inclusions etc.

Scattering centers in a crystal may be observed by shooting a He-Ne red laser beam through the crystal. Fig. 9 shows two photos for SIPAT-LYSO-L8 and SIPAT-LYSO-L9 with the laser beam entering longitudinally from the seed end (right) of the crystals. Scattering centers are clearly visible at the tail end of these crystals. Observations also show scattering centers at the tail end for other crystals with poor longitudinal transmittance. Since the poor transmittance was found at the seed end this observation ruled out macroscopic defects at the seed end. We thus conclude that the poor transmittance in these samples are caused by point defects at the seed end which absorb light.

This issue of the absorption band at the seed end found in SIPAT-LYSO-L7, L8, L9 and L10 was brought to the attention of SIPAT, and was discussed in a site visit. The problem was traced back to a bad seed crystal used in the growth process. After a rigorous quality control for the seed crystals the absorption band at the seed end was eliminated. Fig. 10 show the longitudinal transmittance spectra for eleven LYSO crystals: ten from SIPAT and one from Saint-Gobain. No absorption

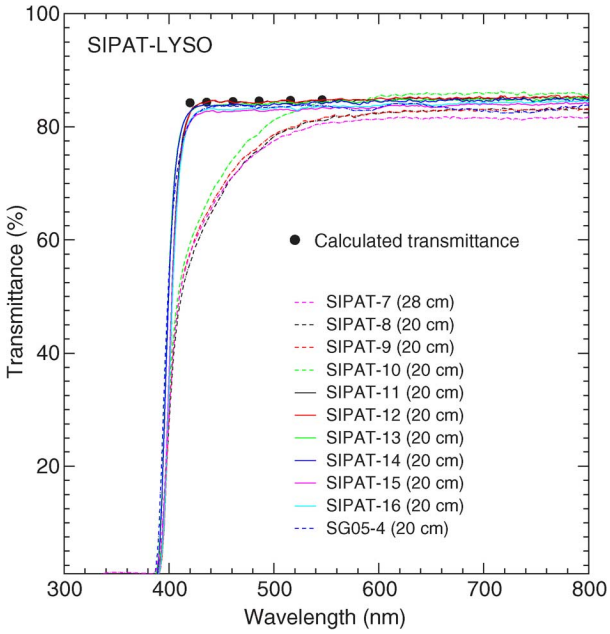

Fig. 10 Longitudinal transmittance spectra are shown as a function of wavelength for eleven LYSO crystals: ten from SIPAT and one from Saint-Gobain.

TABLE I
LIGHT OUTPUT MEASURED WITH HAMAMATSU R1306 PMT FOR SIPAT LYSO SAMPLES

ID	Light Output (p.e./MeV)	Energy Resolution FWHM (%)
SIPAT-7	1380	12.2
SIPAT-8	1330	13.1
SIPAT-9	1450	12.3
SIPAT-10	1490	12.3
SIPAT-11	2010	10.7
SIPAT-12	1970	10.4
SIPAT-13	2050	11.5
SIPAT-14	2100	10.9
SIPAT-15	2040	10.5
SIPAT-16	2050	10.1

was found between 400 nm and 800 nm for SIPAT-LYSO-L11 to L16, which were grown with seed crystals of high quality, and the Saint-Gobain sample. A specification of 75% at 420 nm was introduced to reject crystals with poor longitudinal transmittance. Because of the improvement in optical transmittance the light output of 20 cm long LYSO crystals from SIPAT is 30% higher than that with the absorption problem as shown in Table I. The average FWHM resolution measured by the Hamamatsu R1306 PMT with 0.511 MeV γ-rays from a ^{22}Na source for long LYSO samples have also been improved from $>$12% to better than 11% as shown in Table I.

V. SUMMARY

The first $2.5 \times 2.5 \times 28$ cm (25 X_0) LYSO sample was successfully grown at SIPAT. It has consistent emission, adequate light response uniformity and good radiation resistance against γ-rays up to 1 Mrad.

This sample and three other large size samples from SIPAT, however, showed poor longitudinal transmittance between 400 nm and 600 nm as well as poor transverse transmittance at the seed end. This poor transmittance at the seed end was understood as being caused by point defects which absorb light, and was traced back to a bad seed crystal used in their growth. With rigorous quality control on seed crystals recently grown LYSO crystals show no absorption band at the seed end and have a light output of 30% more than those with this problem. The corresponding average FWHM resolution measured by using 0.511 MeV γ-rays from a ^{22}Na source is also improved from $>$12% to better than 11%.

REFERENCES

[1] C. Melcher and J. Schweitzer, "Cerium-doped lutetium oxyorthosilicate: A fast, efficient new scintillator," *IEEE Trans. Nucl. Sci*, vol. 39, no. 4, pp. 502–505, Aug. 1992.

[2] D. W. Cooke, K. J. McClellan, B. L. Bennett, J. M. Roper, M. T. Whittaker, and R. E. Muenchausen, "Crystal growth and optical characterization of cerium-doped $Lu_{1.8}Y_{0.2}SiO_5$," *J. Appl. Phys.*, vol. 88, pp. 7360–7362, 2000.

[3] T. Kimble, M. Chou, and B. H. T. Chai, "Scintillation properties of LYSO crystals," in *Proc. IEEE Nucl. Sci. Symp.*, 2002, vol. 3, pp. 1434–1437.

[4] J. M. Chen, R. H. Mao, L. Y. Zhang, and R. Y. Zhu, "Large size LSO and LYSO crystal for future high energy and nuclear physics experiments," *IEEE Trans. Nucl. Sci.*, vol. 54, no. 3, pt. 2, pp. 718–724, Jun. 2007.

[5] SuperB Conceptual Design Report, INFN/AE-07/2, SLAC-R-856, LAL 07-15, Mar. 2007C. Cecchi, "A LYSO Calorimeter for the super B factory," in *J. Phys.: Conf. Ser.*, 293 012066.

[6] R. Y. Zhu, "An LSO/LYSO crystal calorimeter for the ILC," in *Proc. 2005 Int. Linear Collider Phys. Detector Workshop 2nd ILC Accelerator Workshop*, Snowmass, CO, Aug. 14–17, 2005, Published in ECONF C0508141:ALCPG0705,2005.

[7] J. M. Chen, R. H. Mao, L. Y. Zhang, and R. Y. Zhu, "Gamma-ray induced radiation damage in large size LSO and LYSO crystal samples," *IEEE Trans. Nucl. Sci.*, vol. 54, no. 4, pt. 3, pp. 1319–1326, Aug. 2007.

[8] R. Mao, L. Zhang, and R. Zhu, "Effects of neutron irradiations in various crystal samples of large size for future crystal calorimeter," in *Proc. 2009 IEEE Nucl. Sci. Symp. Conf.*, 2009, vol. 1–5, pp. 2041–2044.

[9] F. Nessi-Tedaldi, G. Dissertori, P. Lecomte, D. Luckey, and F. Pauss, "Studies of cerium fluoride, LYSO and lead tungstate crystals exposed to high hadron fluences," presented at the IEEE NSS Conference, 2009, Paper N32-3.

[10] R. Mao, L. Zhang, and R. Zhu, "Optical and scintillation properties of inorganic scintillators in high energy physics," *IEEE Trans. Nucl. Sci.*, vol. 55, no. 4, pt. 2, pp. 2425–2431, Aug. 2008.

[11] D. A. Ma and R. Y. Zhu, "Light attenuation length of barium fluoride crystals," *Nucl. Instr. Meth.*, vol. A333, pp. 422–424, 1993.

[12] R. Mao, L. Zhang, and R. Zhu, "Gamma-ray induced radiation damage in PWO and LSO/LYSO crystals," in *Proc. 2009 IEEE Nucl. Sci. Symp. Conf.* , 2009, vol. 1–5, pp. 2045–2049.